DOE/ER/40706--2

Research in Elementary Particle Physics

TECHNICAL PROGRESS REPORT

James R. Bensinger, Craig A. Blocker
Lawrence E. Kirsch, Howard J. Schnitzer

BRANDEIS UNIVERSITY
Department of Physics
Waltham, Massachusetts 02254-9110
June 1, 1993–May 31, 1994

Prepared for the United States
Department of Energy
Under DOE Grant DE-FG02-92ER40706

DISCLAIMER

Portions of this document may be illegible in electronic image products. Images are produced from the best available original document.

TABLE OF CONTENTS

EXPERIMENT

THEORY

TECHNICAL PROGRESS REPORT

June 1, 1993 – May 31, 1994

Under this contract, research has been performed on both theoretical and experimental properties of elementary particles. A brief description of the work which is either in progress or has been completed is given below.

EXPERIMENT

1. INTRODUCTION

The Brandeis experimental particle physics group has for many years pursued an understanding of physical interactions at the highest available energies. To this end we have been active in the development of the Collider Detector at Fermilab (CDF) and in the development of detectors that were planned for the SSC. We have also had an active program of analysis to understand the data and its implications from these detectors.

Brandeis first joined the CDF experiment in 1981. We had major responsibility (along with the CDF group at Harvard) for mechanical design, front end electronics development, construction, testing, and installation of the Forward Electromagnetic Calorimeter. In addition we had major responsibility for the design and implementation of the gas system and of the gas gain monitoring system for the gas calorimeters.

We have fully partaken in the support activities of CDF. We have performed extensive studies of calorimeter energy response, both for the electromagnetic and hadronic calorimeters, and have implemented the results from these studies into the CDF detector simulation software package. We have participated in internal reviews, workshops, code development and evaluation, and assisted other members of the collaboration when ever local expertise and resources made that appropriate.

Brandeis has actively participated in the analysis of CDF data. Early activity included trigger, rate, and decay mode studies for the top quark searches. There were two Ph.D. thesis on searches for the top quark, one on a search in the e-μ channel by Milciades Contreras became the basis for one of the observation channels recently announced by CDF. Other analyses performed by the group have included QCD studies, b-quark studies, and electroweak studies. We have made measurements of the inclusive jet cross section and its evolution with $\sqrt{s}$, and a series of studies involving direct hard photon production is underway. Studies of the b-quark have included $b\bar{b}$ mixing, production cross sections in both the central and forward region, and analysis of various decay modes. We took a leading role in the development of electron identification in CDF and contributed to electroweak physics by measuring the angular asymmetry in Z production and decay at the Tevatron.

While the SSC program was still operational, Brandeis was very active in the development of the Solenoidal Detector Collaboration (SDC) experiment. We participated both in the development of the SSC laboratory itself and the SDC detector. Two of us took leave from Brandeis to further this effort. Professor Bensinger became the SDC Muon Subsystem Manager and Professor Blocker became the task leader for the SDC Calorimeter Calibration Group. Since the termination of the SSC, we have been assisting with the sad duty of orderly termination of the project.

Brandeis remains fully engaged in the understanding of physical interactions at the highest available energies. While pursuing physics analysis, detector support activities and detector upgrades at CDF, we are also exploring the physics potential of the LHC. Pending overall agreements between the Department of Energy and CERN, we have joined the ATLAS experiment at CERN. The expertise gained in planning SSC detectors is directly applicable here. We have been instrumental in organizing a consortium of Boston area Universities (Boston University, Brandeis, Harvard, MIT, and Tufts) to pool our resources to participate in this experiment.

2. CDF ACTIVITIES

The goal of the current run, which began in December of 1993 and is anticipated to continue through June 1995, is to accumulate an integrated luminosity of 100 pb^{-1} in order to enlarge the top quark data sample. The Brandeis group will continue to provide support for the gas calorimetry and shift manpower.

In addition to the top data, we expect to obtain a large increment in the photon plus jets data sample which will enable more detailed studies of these processes.

2.1 CDF System Support

The Brandeis group has been involved with all phases of the CDF detector program since its construction. Early efforts focused on a collaboration with Harvard on the construction of the forward electromagnetic calorimeter. One of the Brandeis commitments was to design and construction of gas distribution and gas gain monitoring system for all the plug and forward gas calorimeters. Maintaining this system has been an ongoing responsibility of the Brandeis group. We have also had major responsibility for establishing the energy response of the CDF calorimeters, both electromagnetic and hadronic.

2.1.1 Gas Gain

The gas gain system of CDF has, among various components, nearly 90 proportional tubes, 200 temperature probes, half a dozen pressure probes and 48 channels of PC controlled high voltage channels. The system was designed to continuously monitor the gas mixture flowing through the forward and plug calorimetry of the CDF detector, while at the same time maintaining a constant gain during fluctuating temperatures and atmospheric pressure. This latter component of the gas gain system, referred to as "feedback," is a new feature of the gas calorimetry system [1]. The complete system is described in detail elsewhere [2].

During the past year, the Brandeis group has been involved in several gas gain projects. With the conclusion of the last data run ("Run Ia" – August '92 to May '93), we spent last summer constructing, calibrating and installing 50 new proportional tubes to be placed throughout the gas calorimetry system. These tubes were replacement tubes for those that had "aged" (deposits forming on the wires that reduced the gains of the tubes during the previous data run). In parallel with tube replacement was a complete rearrangement of the tube ensemble to insure a stable system for the upcoming 12 month run. Each temperature probe was checked for its placement and performance at this time.

The Brandeis group, in collaboration with the MIT group, is entirely responsible for the readout and performance of all proportional tubes; this includes the associated electronics. This is accom-

plished through three techniques. Every two weeks, a complete set of spectra is collected for each proportional tube. These spectra alert the users of potential aging or electronics problems.

As the gas gain system accumulates data continuously, the information is stored in a database. We analyse trends in the gain of the gas calorimeters, as well as individual tube behavior. On a daily basis, we monitor each tube's performance and compare the gain to its historical behavior.

Using the response of the proportional tubes, we have determined the gas gain constants needed for the CDF trigger. This was done in preparation for the current data run.

With the current data run of CDF projected to continue for the upcoming year, the Brandeis group will continue to be involved in the maintenance of the gas gain system. Planned accelerator shutdowns this summer will allow us to replace both defective tubes and temperature probes.

Although the gas gain system was scheduled to be replaced at the end of this current data run, it is not clear that the detector upgrades to replace it will be completed in time. We are already beginning to consider a complete overhaul of the gas gain system in preparation for yet another data run.

2.1.2 New Energy Scale Determination for CDF Jets

By the summer of 1993, various analyses of low-E_t showers in the Central Electromagnetic Calorimeter indicated that CEM response is nearly linear down to energies of order 1 GeV. This result contradicted early predictions from the CDF detector simulation Monte Carlo package. Since this package was used, among other things, to determine the CDF jet E_t scale (the ratio of observed jet E_t to incident E_t) used in the corrections for CDF jet physics measurement, it was necessary for this to be reevaluated.

In addition, the CDF QCD Group requested a change in the definition of jet E_t, namely that the correction applied for the presence of uncorrelated energy ("underlying event", "pedestal effect") be limited to the level of energy density seen in Minimum Bias events. It is well known that the level of calorimeter E_t observed at large angles to jets in jet events is roughly twice that seen in Minimum Bias triggers. Historically, up to this point, CDF jet analyses had considered this large-angle dijet energy as an uncorrelated "energy noise" to the jets. The decision to correct only for the Minimum Bias energy density reflects our belief that the increasingly sophisticated theoretical calculations be held accountable for predicting the difference in non-jet energy seen in jet and Minimum Bias events.

The jet E_t scale was reevaluated, incorporating both changes [6]. Using this new jet E_t scale, CDF's published results for inclusive jet production from the 1988-1989 dataset were updated. These results include: the inclusive cross sections at $\sqrt{s} = 1800$ and 546 GeV, the x_t scaling ratio, and the 546 and 1800 GeV low E_t cross section comparison and cross section ratio. Systematic error on these physics measurements, arising from jet E_t scale uncertainty, was also reevaluated.

2.1.2.1 Hadronic Energy Scale for CDF Central Calorimeters The response of the CDF Central Calorimeter array to hadron energy deposition is crucial for a number of CDF physics measurements (W mass determination which relies heavily on response to low-P_t accompanying energy; the inclusive jet spectrum measurement and the related di-jet invariant mass spectrum measurement; jet fragmentation studies). CDF physics results have emphasized the Central Calorimeter, because of its higher gain stability (scintillator rather than gas) and the ability to compare tracked

charged particles with calorimeter response.

In 1990–91 the response of the Central Calorimeter to hadrons was updated and re-evaluated, based on a Brandeis analysis of 1990 CDF Test-Beam data and re-analysis of Central response to isolated charged particles observed in CDF Minimum-Bias data [9].

In the Fermilab Test-Beam data, all three calorimetry systems (Central, Plug, and Forward) were studied with pions and electrons; pion momentum ranged from 7 GeV/c to 227 GeV/c. The linearity of average Central Calorimeter response to π's was determined, while a separate study looked in detail at response (to both π's and e's) in the cracks between central modules [10]; new information on both response and energy resolution, and their energy dependence, was obtained.

Particle momenta below 7 GeV/c were not obtainable in the 1990 Test-Beam, and yet this particular interval is crucial to CDF jet studies, to the W mass measurement, and to top quark decay into jets. Response to π's below 7 GeV/c was determined in-situ using particles tracked by the Central Tracking Chamber (CTC) in CDF minimum bias data (events with any evidence of inelastic $\bar{p}p$ collision). Tracks were extrapolated to the Central Calorimeter, and a comparison of CTC momentum to calorimeter energy was made. A subtraction was made on a statistical basis for accompanying neutral (π^0) energy, based on a study of Central Electromagnetic (CEM) energy deposited outside the CEM target tower.

The measured response to very low energy hadrons (0.75–3 GeV) was observed to be only 60% of measured momentum, compared to the (face-averaged) result for 7 GeV/c Test-Beam pions of 80%. The sample of isolated tracks extended to 25 GeV/c, where results were seen to agree well with test-beam measurements.

Results for response and resolution were incorporated into the CDF detector simulation software package [11].

2.1.2.2 CDF Response to Low Energy Jets

The substantial branching ratio for the decay of the top quark into lepton + jets helped to motivate a study of CDF's response to low transverse energy jets ($E_t < 30$ GeV). The definitive set of studies of low E_t response was conducted at Brandeis. The CDF Monte Carlo detector simulation was tuned to reflect Test Beam information on response to single pions and electrons. A sample of 1.8 million Monte Carlo jet events was then generated and simulated, and analyzed to establish predictions for the low E_t jet response in the detector. Information on the absolute jet energy-scale and its systematic error was derived from this sample. Jet E_t resolution was also studied and parametrized.

The information obtained from this series of studies was supplied to various CDF analysis efforts, including the jet multiplicity observed in W events, and a kinematic-constraint analysis of candidate top→lepton+jets events [7]. For both these analyses, the understanding of jet E_t systematic error and resolution was crucial.

2.2 Physics Analysis

The physics interests of the group have varied over a wide range of topics, including earlier work on top searches, electroweak physics, inclusive jet production, scaling behavior of jets, $b\bar{b}$ mixing, b quark production, and leptoquarks to more current work of top kinematics, ψ production, and a

variety of measurements associated with photon plus multijet channels.

2.2.1 Photon + Multijet Analysis

The physics potential at hadron colliders includes detailed measurements of proton substructure and tests of the standard model. The event sample consisting of an isolated photon plus two-or-more jets is especially well suited for these studies.

The large $\sqrt{s}$ available at the Tevatron collider gives access to the behavior of the proton structure function in a region of parton fractional momentum (x) and energy transfer (Q^2) inaccessible at other experiments: realistically achievable trigger thresholds of the order of 10 GeV for the final-state allow the structure function to be probed to x values as small as 10^{-2}–10^{-3}. The gluonic part of the proton structure function dominates in this region of x and is also the least understood theoretically. Measurements of this very low-x gluonic structure function are important for pinning down QCD hard-scattering predictions, for testing the Altarelli–Parisi scaling prediction, and for extrapolating interaction cross sections to colliders at higher $\sqrt{s}$.

Direct (*i.e.*, prompt) photons can be produced in $\bar{p}p$ collisions through the Compton process ($q+g \rightarrow q+\gamma$) and $q\bar{q}$ annihilation ($q+\bar{q} \rightarrow g+\gamma$). The photon + X final state is particularly useful in that one leg of the hard scattering is measured extremely well ($\sigma \approx 15\%\sqrt{E_t}$) down to E_t's of 5–10 GeV; by contrast the energy measurement of low-E_t jets is poor ($\sigma \approx 100\%\sqrt{E_t}$) due to hadron resolution and jet fragmentation effects. The good photon E_t measurement, along with precise angular measurements of the recoil jets and the assumption of transverse momentum balance, enables a clean determination of the CM energy and thus $\sqrt{x_1 x_2}$. Given a theoretical prediction for the direct photon matrix element, information on the low-x structure function can be extracted.

2.2.1.1 Photon + 2 Jets: Bremsstrahlung Production

A difficulty with measuring the direct photon cross section at low E_t^γ is the presence of direct photons from bremsstrahlung off initial- or final-state quark lines. Theoretical uncertainty on the contribution of these diagrams is large, and introduces a corresponding uncertainty into predictions of direct photon production. Bremsstrahlung photons contribute more at low E_t^γ and therefore limit our understanding of the gluon structure function at the lowest-x values probed by the CDF direct photon measurement. Insight into the physical bremsstrahlung process can come from a study of the photon + 2 jets final state. This sample consists of some mixture of events in which gluonic radiation was produced in conjunction with a direct photon hard-scatter, and events in which a bremsstrahlung photon was radiated from a quark hard-scattering. The topologies for these two classes of photon + 2 jet events are different, and thus the magnitude of bremsstrahlung process can be extracted by a study of this data. Variables with distinguishing power for gluon radiation vs. bremsstrahlung include the angle between the photon and the lower E_t jet, $\cos\theta^*$, and the E_t spectrum of the lower E_t jet relative to that of the photon.

The CDF photon data currently being examined for this analysis represents an integrated luminosity of 19nb^{-1} taken during the 1992–93 run. The event trigger required a cluster in the Central Electromagnetic Calorimeter (CEM) above 16 GeV, with less than 4 GeV of calorimeter E_t in an annular region centered on the cluster. Off-line, a statistical separation of direct photons from background (merged photons from π^0 decays from jet fragmentation) is obtained using the transverse shower profile in the CEM or the fraction of candidate clusters which shower early in the Central Pre-Radiator chambers located upstream of the CEM. The purity of the sample is E_t^γ-dependent

but is roughly 10%.

Jets in these events are identified using the standard CDF clustering algorithm, which defines jets based on calorimeter E_t observed in a cone in $\eta - \phi$. A cone radius of 0.4 is used to allow small photon-jet angles. Furthermore, jets are restricted to lie within the Central or Plug Calorimeters ($|\eta|$ <2.5), and have E_t >8 GeV. Two or more jets are required.

A total of 24,300 events pass all requirements. In Fig. 1 we show the distribution of the $\eta - \phi$ separation (δR) between the photon and the lower E_t jet. The isolation cone around the photon excludes the region $\delta R < 0.7$. Also shown is a prediction from the PYTHIA QCD shower Monte Carlo, broken down into bremsstrahlung and non-bremsstrahlung components. The enhancement observed at δR between 1 and 2 earmarks the presence of bremsstrahlung photons. Work is in progress to correct this and other distributions for detector effects, and to compare them with theoretical predictions.

2.2.1.2 Photon + 2 Jets: Color Coherence

On a second front, the photon + 2 jets data sample is also being investigated for the presence of QCD color-coherence ("string") effects. CDF has recently observed color coherence effects in tri-jet events, arising out of destructive interference between initial- and final-state gluon radiation. This interference manifests itself as a suppression of radiation outside a cone centered on the beam-line and bounded by the radiating jet. Color coherence in the photon + 2 jets sample is expected to be stronger than in the tri-jet data (all non-bremsstrahlung graphs for direct photons are color-connected between the initial and final states), but may also take on a different character.

2.2.1.3 Photon + 3 Jets: Double Parton

The studies of the proton structure function outlined above can be extended into new territory by an analysis of the dynamics of *two* hard scatterings in one $\bar{p}p$ collision. Double Parton (DP) scattering produces a final state that mimics a combination of two independent scatterings. Using the 1989 data, CDF searched for DP events in the 4-jet final state, and found some evidence for their presence at the level of $5.4^{+1.6}_{-2.0}$% of the events; the remainder of the events were consistent with QCD predictions of double gluon radiation from a strong 2→2 hard scattering.

A better signal-to-noise for DP is obtainable in the photon + 3 jets data sample. For this final state the DP cross section can be thought of as being a product of the photon + 1 jet cross section and the di-jet cross section. The background QCD process for photon + 3 jets, double gluon radiation from photon + 1 jet, is roughly proportional (K-factor) to the photon + 1 jet cross section. Thus "signal-to-noise" roughly goes as the di-jet cross section itself, which is large for low jet E_t. Unlike the CDF 4-jet trigger, the photon trigger places no requirement on the jets accompanying the photon. Jets in the former analysis were required to be above 25 GeV, jets in the latter are accepted above 8 GeV; the di-jet cross section at the latter E_t is approximately 60 times higher than at the former.

Variables that segregate DP from QCD background take advantage of the individual momentum balance of each of the two hard-scatterings, and the independence of the scatterings. The variable S represents the significance away from the hypothesis that photon + 3 jet events consist of two pairs (a photon + 1 jet and a di-jet), each of which balances transverse momentum. The δS variable is the angle in the transverse plane between the resultant P_t vector of each pair: in DP events this angle is randomly distributed, while in QCD events momentum conservation biases this angle

towards 180°.

The CDF data sample under investigation for this analysis is the same as that described above, with the requirement that three or more jets pass the selection cuts, yielding a total of 7450 events. To obtain a theoretical prediction for photon + 3 jets, we are working with Alan Stange, a Brookhaven theorist to implement and improve his Lowest Order (L.O.) QCD calculation, the first of its kind for this process.

Fig. 2 compares the δS distributions for the data, a QCD prediction from PYTHIA, and a Monte Carlo DP sample (detector simulation has been applied to the latter two samples). The data exhibits a flatter distribution for δS than does the QCD prediction, and is better fit with an admixture of DP events. Work is proceeding to confirm this early indication of the presence of Double Parton scattering in our data.

2.2.2 Top Kinematics

The top quark is one of the major missing pieces of the Standard Model. CDF has recently submitted for publication preliminary evidence for the top quark based primarily on an excess of the bottom quark jets in W + jets events produced in $\bar{p}$p collisions.

It is important to establish whether this excess bottom quark production is due to the top quark or not. One way to due this is to study the kinematics of the jets that accompany the W. The primary background is QCD production of jets in W events, in which the transverse energy (E_t) spectrum of the jets is expected to be soft (that is, to peak at any E_t cut that is made) due to the infrared divergences of QCD. On the other hand, the E_t scale for jets from top production is related to the mass of the top quark. If the top quark mass is sufficiently large (above roughly 120 GeV/c^2), the jet E_t spectra can be used to separate top events from background.

One of the difficulties of identifying top events is their complexity. For example, top events with one semileptonic decay yield a lepton, a neutrino (detected as missing E_t), a b quark jet, a $\bar{\text{b}}$ quark jet, and two light quark jets. This means there are a large number of jet kinematic distributions that can be used to separate top and background. Many of these have been studied. The limited statistics and uncertainties in the background make a definite confirmation of top production difficult, but there are many indications that there are top events in the CDF data sample. For example, Fig. 3 shows a scatter plot of the second and third highest jet E_t's (E_t^2 versus E_t^3) for the ten W + 3 jet events tagged as having at least one bottom quark jet. The line divides the Monte Carlo background data into equal samples. The data are clearly distributed towards higher E_t (eight out of ten events on the higher E_t side of the line), but the statistics are obviously limited. Many other distributions (such as the number of 4 jet event and the E_t spectrum of the fourth jet) show a similar behavior, that is, they favor the top quark interpretation, but the limited statistics make it difficult to make a definitive statement. Obviously, an increase in the data sample is needed to understand these events.

2.2.3 Central b Quark Production

The CDF collaboration has measured the single inclusive bottom quark cross section in a number of ways, including inclusive electrons, ψ's, events with an electron and a D*, and exclusive B decays. Although all of these measurements have relatively large errors, they tend to measure a cross section that is significantly higher (roughly a factor of two) than the theoretical prediction.

To try to understand whether this discrepancy was due to experimental systematics, we measured the bottom production cross section by a method that should have much different systematics, namely, by looking for events where both the b and $\bar{b}$ decay semileptonically. By selecting events events with an electron and a muon, a relatively clean measurement can be made. The major disadvantage to this method is the limited statistics due to requiring two semileptonic decays.

The correlated $b\bar{b}$ cross section was measured as a function of the P_t cuts on the b and $\bar{b}$. When this cross section is converted to an equivalent single inclusive b cross section, results consistent with previous CDF measurements and higher than the theoretical prediction are obtained as shown in Fig. 4.

2.2.4 Forward b Quark Production

Jodi Lamoureux, who recently joined the Brandeis group, has continued her work on the measurement of the bottom quark production cross section using forward muons. This work was presented at the April 1994 meeting of the American Physical Society and also at a Fermilab Seminar on May 10 of this year. The inclusive cross section for bottom quarks with $P_t^b > 20$ GeV/c and $1.9 < |\eta^b| < 2.5$ is $(79^{+12}_{-15}\ ^{+31}_{-23})$nb compared to the theoretical prediction of $(21.3 \pm 0.4^{+10.2}_{-5.9})$nb. The correlated cross section for bottom quarks with $P_t^b > 20$ GeV/c, antibottom quarks with $P_t^{\bar{b}} > 15$ GeV/c and $1.9 < |\eta^b| < 2.5$ is $(59^{+10}_{-13}\ ^{+24}_{-17})$nb compared to the theoretical prediction of $(9.3 \pm .9 \pm 1.8)$nb. Both results are within 2.5σ of theoretical predictions and are consistent with the central CDF results projected to forward pseudorapidity.

The CDF bottom quark production cross section measurements have so far shown that either some tuning of the gluon structure function is needed in the x region (typically .01 or so) which CDF measurements probe or that the theoretical calculation is highly uncertain. Through the correlated bottom quark measurement the primary scale factor (μ) which is used to renormalize the theoretical calculation can be set to a meaningful value and a more restrictive theoretical comparison made. Furthermore, the forward cross section is more sensitive to changes in the gluon structure function than the current central measurements. The bottom quark system is a good laboratory to search for further tests of QCD and increase our understanding of the gluon structure of the proton.

As CDF accumulates more data, improved measurements in this region will be possible. There are two forward bottom quark measurements which are being pursued at CDF, one from a J/ψ and Υ data set and the other from a muon + jets data set. We have a lot of expertise in this area and we expect to participate in future studies of forward bottom quark production.

2.2.5 ψ' Production

Charmonium production is currently the best way to study b-quark production at CDF at the lowest possible transverse momentum of the b. While the signature and signal-to-noise for the J/ψ are excellent, the actual conclusions regarding b production are strongly dependent on the fraction of the data sample due to b decays. In contrast, conventional wisdom has it that ψ''s ($\psi(2s)$) are produced only by B decays.

In the course of this analysis, a very large prompt (zero-lifetime) component for the observed ψ' signal has been seen. This is contrary to the theoretical expectations of up to a year ago, which indicated that direct ψ' production should be insignificant when compared to that from B decays.

The production mechanisms and cross section of the ψ' were studied by examining $\psi' \rightarrow \mu^+\mu^-$

events in the CDF data. Fig. 5 is the $\mu^+\mu^-$ invariant mass distribution in the ψ' mass region. The goal of the study is to discern differences between the two production mechanisms for ψ': one due to B decays and the other due to direct production. To achieve these goals, three pieces of information were used: (a) the ψ' lifetime distribution, (b) the ψ' P_T spectrum and (c) the ψ' isolation.

In order to determine the fraction of ψ''s that result from the decay of B's, the proper time distribution of those events that contain a ψ' were studied. Using the beam center as the primary vertex and the intersection of the two muon tracks as the secondary, the transverse decay length (l_{xy}) could be determined. To convert l_{xy} into a proper time we need to know the P_T of the B, as well as the angle between the B and the ψ'. This has been accomplished with Monte Carlo data. Using maximum likelihood techniques, we fit the lifetime distribution as a sum of signal (B decays) and background (prompt) events. Fig. 6 shows the proper time distribution of ψ' events, as well as the results of the likelihood fit. The fitted B fraction is only 22.6±3.5%, which is considerably lower than the nearly 100% predicted by theory.

By making detailed studies of the ψ' acceptance, the dimuon trigger efficiencies and analysis cut efficiencies, we determined the ψ' cross section to be:

$$\sigma(\bar{p}p \to \psi',\ 4\ \text{GeV/c} < P_T^{\psi'} < 20\ \text{GeV/c},\ |\eta| < 0.5 \cdot Br(\psi' \to \mu^+\mu^-)) =$$
$$0.603 \pm 0.046\ (\text{stat}) \pm 0.066\ (\text{syst})\text{nb}\ .$$

This cross section is a factor of 7 larger than current theoretical expectations.

In order to determine the cross section of ψ''s from B decays, the prompt component of the ψ' data was removed by a large vertex separation cut. Using this approach, we obtain an integrated cross section:

$$\sigma(\bar{p}p \to bX,\ |\eta^b| < 1.0,\ P_T^b > 6.2\text{GeV/c}) = 11.13 \pm 2.37(\text{stat}) \pm 1.89(\text{syst}) \pm 3.34(\text{BR})\mu b\ .$$

This is in good agreement with the upper limit of QCD predictions for b production.

This analysis [14] was performed with the MIT Group and will continue with the data obtained in the current CDF data run, where a data set nearly five times larger than that used in this analysis will be obtained.

2.2.6 Di-jet Differential Cross Section

As another probe of the proton structure function, a project has been undertaken to study the dependence of the di-jet cross section, as a function of jet E_t, on the angular distribution of the second jet [5]. In 1992–93 CDF events with two or more jets, the leading pair of jets was examined; events were classified by the relative rapidity of the lead pair ($\Delta\eta$). For each of five $\Delta\eta$ intervals, we evaluate the corrected inclusive di-jet cross section, $\frac{d^3\sigma}{dE_t d\eta_1 d\eta_2}$. Being functions of both E_t and relative rapidity, these cross sections are sensitive to the proton structure function (constraining both $\sqrt{x_1 x_2}$ and $x_1 - x_2$). For the actual figures of merit in this analysis, we take the ratio of each of these cross sections (as a function of E_t) to the di-jet cross section where both jets are in the central rapidity interval. As seen in the jet scaling analysis, systematic error in both measurement and theory are reduced in the ratio. We find that the agreement between our data and QCD predictions using the Lowest Order structure functions of Morfin and Tung is good.

Work is ongoing to test the predictions from the more sophisticated Next-to-Leading Order (N.L.O.) structure functions. This analysis is also being extended to include CDF data being taken in the current Tevatron run.

2.2.7 Jet Scaling Analysis

An extensive analysis of the scaling behavior of jet production, conducted at Brandeis using CDF data taken at two collision energies, was completed at the end of 1992. Results were published in the 8 March 1993 issue of *Physical Review Letters.*

The naive "scaling" hypothesis predicts that "dimensionless" jet production cross sections should be independent of $\bar{p}p$ collision energy. The more realistic QCD hard scattering calculations predict nonscaling behavior, resulting from the evolution of the proton structure functions and the running of the strong coupling constant, α_s.

CDF inclusive jet data from Tevatron runs at $\sqrt{s}$=1800 GeV and 546 GeV were used for this analysis. Our corrected results for the 546 GeV inclusive jet cross section agree well with measurements from UA1 and UA2 at CERN, when similar definitions of corrected E_t are applied.

The ratio of the dimensionless invariant cross section at 1800 GeV to that at 546 GeV, R, was used as a measure to test scaling behavior. The total systematic uncertainty on this ratio is approximately $\pm$15%. The deviation of our measured ratio from the scaling hypothesis (R=1) was tested by comparing the average value of R against unity. The average R for our data, constructed in a weighted fashion using statistical and systematic errors, is $1.51\pm0.04\pm0.21$. Comparing the data average to the scaling prediction yields a confidence level of 1.7%, from which we conclude that scaling in jet production is excluded by our data.

Our measured R data was also compared to N.L.O. QCD calculations for a variety of structure functions and choices of renormalization scale (Q^2). Predictions for average R range from 1.83 to 2.01, and thus lie 1.5–2.4 σ above our data. This poor level of agreement with NLO QCD has generated definite interest in the theoretical community. Communication is continuing with Steve Ellis, Davison Soper, and others in the theoretical community, in an attempt to understand the jet scaling result [8].

2.2.8 Measurement of the Inclusive Central Jet Cross Section and Quark Compositeness Limit

Brandeis produced the corrected inclusive jet cross section result from the 1989 CDF data-set, as part of the jet scaling analysis [12]. For the 1992–93 data, we are working with Anwar Bhatti at Rockefeller University who is producing the inclusive spectrum and a new limit on hypothetical quark compositeness. Work on extracting the quark compositeness limit is ongoing, and includes understanding the effects of multiple $\bar{p}p$ collisions in the new high-luminosity Tevatron environment.

The inclusive cross section for jet production as a function of jet E_t provides a measure both for "standard" physics (including tests of the QCD predictions for the quark and gluon structure functions at 1800 GeV) and possible new physics (quark compositeness). The actual measurement is complicated by the fact that the jet energy spectrum is a steeply falling function, behaving approximately as the fifth power of the jet transverse energy. As such, the measurement of this cross section is extremely sensitive to the knowledge of the jet energy scale, and to resolution effects. Due to the presence of calorimeter energy losses (cracks, leakage, and low-p nonlinearity),

corrections must be applied to observed jet energies. These corrections come from Monte Carlo simulations tuned to reproduce the calorimeter response measurements discussed above. Also since calorimeter nonlinearity introduces a correlation between measured energy and jet fragmentation, the Monte Carlo was tuned to reproduce the fragmentation properties observed in CDF's jet sample [3]. Jet E_t resolution was determined from our tuned Monte Carlo and checked against momentum balance observed in CDF di-jet events [4].

The resulting analysis of inclusive jet data for the 1988–89 CDF run produced a cross section spanning nearly 8 orders of magnitude in rate, with jet E_t extending to 425 GeV. Systematic error on the cross section (primarily from energy scale and resolution uncertainties) was reduced by a factor of two over the earlier (1987–88) analysis of 1987 CDF data.

3. SSC ACTIVITIES

The Brandeis group was very active in the development of the Solenoidal Detector Collaboration (SDC) experiment. At Brandeis we worked with Harvard and Tufts on detector development for the SDC muon system. Professor Bensinger became the SDC Muon Subsystem Manager and as such he had responsibility for the overall development of the muon subsystem. Professor Blocker became the task leader for the SDC Calorimeter Calibration Group. Since the termination of the SSC, both professors Bensinger and Blocker have been assisting with the unpleasant duty of closing down the project.

3.1 SDC Muon Subsystem

The muon measurement system is based on drift tubes determining the tracks before and after a large toroidal magnet. The production of drift tubes and assembly into modules for the SDC muon system was divided regionally: barrel, intermediate, and forward. These detectors along with scintillation counters and alignment system were to be produced by various university groups along with Russian and Japanese collaborators. Professor Bensinger was the lead physicist for the design and fabrication of the muon toroid magnet. In addition he was responsible for developing the organization of the measurement groups, setting overall directions, reviewing the progress of the groups, tracking the development of the muon system design, planning for future activities including manpower and budgets, and developing the muon subsystem contribution to the SDC integrated project schedule.

3.1.1 SDC Muon Magnet Development

The muon barrel toroidal magnet was to be built from 196 iron blocks, approximately 100 tons each, bolted together. The toroid sits on a support structure designed to have a minimum of solid angle and to accommodate both long term floor motion and short term motion from the movement of the calorimeter and forward muon toroids into the barrel toroid. The magnet was being designed by a team of engineers from the SSCL, Fermilab, PSL (Wisconsin), and JINR (Dubna). We planned to build the magnet with steel from Novolipetsk with the block fabrication at Atommash, both plants in Russia.

By the time of the termination of the SSC, we had validated the large block bolted design. This approach had the advantage of a quick, easily certified assembly, and appears to be a very reliable design. It was tested by building two full sized blocks for the magnet, bolting them together, and

measuring the bolt elongation under stress. The results of these test were in complete agreement with the design calculations. The coil design was innovative and again had a quick, certifiable assembly. Substantial progress was made in chemistry and material specifications for Russian steel to be used in the magnet: We also confirmed that the Russian suppliers were able meet our specifications and we developed working relations with personnel in both Atommash and Novolipetsk.

To insure the progress of the work, weekly video-conference engineering meetings were held and several trips to Russia were made to visit laboratories and manufacturing facilities. At the end we had completed and validated the design. We were preparing for a critical (final) design review.

3.1.2 Detector Development

The drift tube design for SDC was novel and had the promise of a large scale precision system. We undertook studies of gas leaks, crimping, and wire tension, wire positioning, and production line development for the drift tubes. It was intended that the initial tube assembly facilities would be in Seattle and the Boston area. Brandeis had major responsibility for the development of the Boston production facilities.

This activity was also supported by a small grant from the Texas National Laboratory Commission (TNRLC). We were joined in this work by Professor Wellenstein of Brandeis who has a background in atomic physics and most recently has been working on a measurement of the neutrino mass using the end point of the β decay electron spectrum. Professor Wellenstein has long experience in detector development and he played a substantial role in this effort.

3.1.2.1 Gas Leak Rate and Back Diffusion Studies

The SDC muon system required tight tolerances on the purity of the Ar-CO_2 mixture of the drift tubes. This required a careful design and testing of the end cap seal and its feedthroughs. The technique of pressurizing the muon tubes and monitoring the gas loss was impractical. Hence a "leak testing hood" was designed to fit over the end of the tube. This hood allowed a small volume (0.1 liter) to be evacuated in seconds, then sealed off. By observing the increase in pressure over time resulted in a leak test 10^6 times more sensitive. Leak rates of less than 2×10^{-5} torr $\times$ liters/sec were achieved.

The muon tubes were always to be kept above ambient pressure, therefore impurity gases cannot leak into the tubes directly but air can diffuse into the tube against the outflowing Ar-CO_2 mixture. This back diffusion was investigated by using a muon tube with an end cap with a leak rate of 2×10^{-3} torr $\times$ liters/sec and filled with pure argon to 50 torr above atmospheric pressure. Then through a leak valve, the nitrogen and oxygen concentration was monitored by a residual mass spectrometer. Results indicated that the back diffusion rate (into the tube) is about 20 times less than the vacuum leak rate (out of the tube) and that it is largely independent of the tube over-pressure.

3.1.2.2 Wire Tension Studies

The SSC muon chambers were expected to have been constructed and installed over a five year period, and then to remain active for at least an additional ten years. The SDC drift tube design utilized a 90 micron diameter tungsten anode which could be up to 9 m long and supported only at its ends. The required tension of 980 gm was about 90% of the elastic limit whereas drift tubes in the past were typically operated at 80% or less. These stringent operating conditions made it

imperative that both the short and the long term behavior of the wire be well understood.

A program was undertaken to attempt to measure both the rapid variation in the wire tension as would occur during construction as well as longer term variations to whether an over tensioning procedure would result in more uniform behavior. Two techniques were developed for rapid *in-situ* measurement of the tension. The first required the use of a permanent magnet placed near the center of the wire. A voltage pulse applied to the wire caused it to vibrate, and the induced voltage could be sensed as a function of time. Fourier analysis of the resulting wave form enabled a determination of the fundament frequency, and hence the tension. A simpler method, which created less disturbance to the wire, was to attach a load cell to the wire which directly measured the tension.

Although the original impetus is no longer present, the technique is being refined to control the temperature and other external variations, so that the data will be made available for the design of future detectors.

3.1.2.3 Drift Tube Wire Position by X-ray Photography

After the assembly of a muon tube the tungsten wire has to be known to a tolerance of 10 to 20 microns with respect to the tube or its supports. Hence it essential that this position is verified at least as a "spot check" during tube fabrication. We developed a test station consisting of a dental X-ray head, fiducial wire system, and dental X-ray film. This system was first applied to the muon tubes designed by Brandeis, Harvard, and Tufts by using a "X-ray clamp" with eight fiducial wires which seated itself onto the two locating grooves at the bottom of the tubes. With two orthogonal pictures taken the wire position was determined to better than 4 microns. Using this device errors in the tube fabrication method were found and corrected.

The system was subsequently adapted to the SDC Muon system by placing the eight fiducial wires into a "X-ray hood" which seated itself onto and over the end caps of the tube using fixtures similar the ones used in the mounting of the tube. An extensive investigation showed that the alignment of the muon tube itself was very important. The device will be used for the 60 muon tubes to be assembled in Boston as part of the SSC close out.

We also have explored a fast "on line" technique using a X-ray vidicon camera and frame grabber so that the wire position can be verified without having to wait for the film development and scanning of the lines. This will be a cost effective method if a large number of tubes have to be tested.

3.1.2.4 Tube Production Facilities Development

The SDC Central Muon System was to be comprised of some 58,000 drift tubes to be manufactured at several different sites. Hence it was important to quickly assemble and test these tubes in a production type facility permitting the use of semiskilled personnel but producing a high quality product. The Brandeis group was responsible for the tooling, instrumentation, and human factors design associated with the manufacture of an estimated 10,000 muon tubes for the SSC. The Boston area SDC muon group had created factories at Tufts and Harvard for this purpose. The goal was to design tooling and automation to rapidly produced tubes meeting quality specifications. Toward this end, we designed automated systems to identify the tubes; transport, tension, and crimp the wires; and provide thermal insertion of the endcaps. We built a Tube Assembly-Test Station which permitted all operations on a single work table. Wherever feasible the operation was automated and

PC controlled and at the same time established a database for each tube. In addition, we developed tools for automated checking of the leak rates of the tubes. All components of the systems were constructed and tested for small samples of tubes, however no large scale production ensued.

3.1.2.5 Alignment Devices

In large detectors there are two facets of detector alignment about which one has to be concerned. First is the placement precision of detector modules, which is set by the precision needed to make the trigger work and to be sure that alignment system sensors or other devices are "within range". Typically the accuracy required is of the order of millimeters. Second is the knowledge of the position of the detector modules, which must be sufficient to achieve the required measurement accuracy in the analysis of data, typically a hundred microns.

By the termination of the SSC project, the design of the SDC alignment system was roughly 85% complete. Many institutions participated in this work including Brandeis, Harvard, Fermilab, and two industrial collaborators; C. S. Draper Laboratory and Precision Systems. Initial prototypes of devices to measure deviations from straight lines (Straight Line Monitor or SLM) over distances greater than achieved by previous devices, performed satisfactorily. An innovative laser ranging system (Range Emitter Receiver or RER) was functioning in a 'breadboard' state and the mechanical design has begun. A prototype analysis model was created revealing insights into the design of the system. Because of the applicability of these devices to LHC experiments we are continuing the development of the RER and SLM systems.

3.2 SDC Calorimeter Calibration Task

One of us (Prof. Blocker) during a leave of absence at the SSC Lab was the Calibration Task Manager for the SDC Calorimeter group. The SDC calorimeter was to use scintillating tiles with wavelength shifting fibers for the sampling medium. This technology requires an extensive calibration system to set the initial energy scale accurately and to precisely monitor drifts in the calorimeter response. The job of the Calibration Task Manager was to oversee the work being done on the calibration system and insure that the system was evolving within the budget and schedule constraints. This system was being developed by Argonne National Lab, Fermilab, Lawrence Berkeley Lab, Purdue University, SSC Lab, and the University of Texas at Arlington.

In addition, Professor Blocker was the head of the SDC Calorimeter Group at the SSC. This group worked on various aspects of the SDC calorimeter, including simulations, calibration tests, calibration design, optics, and phototube studies.

4. LHC/ATLAS ACTIVITIES

Since the demise of the SSC, the most promising facility for studying and understanding electroweak symmetry breaking is the Large Hadron Collider (LHC) being planned at CERN. We have been meeting with other Boston area university groups that were active in the GEM and SDC muon subsystems, to discuss participation in the LHC program. In particular we reviewed the relative physics capabilities of the ATLAS and CMS detectors proposed for the LHC at CERN. These meetings included Boston University, Brandeis University, Harvard University, Massachusetts Institute of Technology, and Tufts University. It was concluded at these meetings that the ATLAS experiment offered the best opportunity for us to pursue the physics goals that we had hoped to pursue at

the SSC. This was an overwhelming conclusion after substantial deliberations. Because of the close proximity and variety of resources available at different institutions, we have a unique opportunity to work together and make a significant contribution to the LHC program. The primary interest of this group is muon systems, but we expect to contribute in other areas as well.

4.1 Muon System Development

The activities of the Brandeis group as part of the ATLAS Boston Muon Consortium include possible contributions in many of the area's of expertise that were developed as part of our participation in the SDC muon system. Areas such as alignment, drift tube R&D, trigger development, electronics and signal processing, and simulations. We are exploring with the ATLAS collaboration which of these activities can be most effective pursued by our group.

4.2 Calorimeter System Development

Another aspect of the ATLAS detector that we are also pursuing is the hadron calorimeter, which will use scintillating tiles with wavelength shifting fibers as the sampling medium. This technology is very similar to that planned for the SDC detector at SSC, and hence the Brandeis group has a great deal of expertise in this area.

The Brandeis group is looking into working on the ATLAS hadron calorimeter with other U.S. high energy physics groups, such as Argonne National Lab, University of Chicago, University of Illinois, and Harvard University. To effectively participate and contribute to ATLAS, it is important that this group work coherently on some aspects of the hadron calorimeter. At this point, it appears that mechanical design, optics, electronics, and simulations are areas where significant contributions can be made.

5. DPF STUDY – WORKING GROUP 10

The Division of Particle and Fields (DPF) of the American Physical Society, in response to the difficulties faced by our field, organized a Long Term Planning Study "To articulate the broad range of physics questions that exist in each [of 10 different] areas, to discuss the means by which these questions might best be addressed, and to relate these means to the exploitation of existing and future facilities both in the United States and in the rest of the world."

This study was organized into working groups with Working Group 10 devoted to a review of Particle Detectors. Professor Bensinger was selected to be one of the co-conveners of this group. The goals of this group is to assess the likely detector technology needs of ongoing and future high energy physics experiments. The role of existing and nascent technologies will be considered. The way in which new detection techniques evolve from the conceptual stage to full scale implementation in working experiments will be studied. This will be done with an eye toward identifying ways in which this process can be aided. For example, an effort will be made to evaluate the extent to which generic detector R&D represents a cost-effective mechanism for stimulating and fostering the development of new techniques.

To achieve these goals we have organized 6 subgroups, each with a different subsystem responsibility. Each of these subgroups will produce the following: (1) Summary of past progress, mode of operation, and current status of detector technology development. (2) Summary of the likely

detector technology needs of current and planned experiments. (3) Recommendation on how to address these identified needs and how to foster refinement of existing techniques and development of new technologies.

The results of the efforts of this working group will be presented at the DPF meeting in Albuquerque this August.

6. BRANDEIS COMPUTING SYSTEM DEVELOPMENT

Computing systems in HEP are entering an era of uncertainty which has not occurred since the introduction of the VAX architecture by DEC in 1978. This processor family and the associated VMS operating system were rapidly adopted by the high energy community and have been the standard ever since. During the last few years, the development of high performance RISC processors have eclipsed that of the VAX CISC architecture leading to the adoption of a variety of modestly incompatible UNIX based systems. DEC has responded by introducing the Alpha processor and a variant of VMS, however there is a strong movement toward UNIX based systems. The issue is further complicated by the fact that the complexity of most HEP code is quite high, and one is dependent on standards for both production and receipt of code needed for analysis. Finally the power engendered by a small number of workstations connected by X-terminals reduces the hardware maintenance cost while providing a level of local computing which is adequate for secondary analysis although inadequate for processing of raw data. The model that evolves therefore should place more emphasis on communications, local storage, and compatibility rather than the model of the preceding years which encouraged expensive local workstations as replacements for even more expensive central processors.

A related problem to the demise of the VAX/VMS is the decline of DECNET as the principal network for HEP. The use of TCP/IP protocols requires increasing the address space in a domain already heavily utilized in the University, thus requiring new subrouting arrangements. Communications in the future will become a more important factor than it already is. The few sites which supported video teleconferencing will be expanded to support other forms of long distance interactivity. We are currently working with the networking group at Fermilab to evaluate lower cost alternatives. This will put more pressure on university backbones, and may require the use of ISDN or other direct services.

Our strategy for the immediate future is to replace our aging and high maintenance cost VAX 3200 workstations with two Alpha systems, and an appropriate number of X-terminals. The CDF strategic plan calls for continued support of OpenVMS on the Alpha platform, since this is the only cost-effective option to continue VMS support. Over time if HEP abandons VMS, these systems can run OSF/1, the DEC flavor of UNIX. Our immediate goal is to provide sufficient computing power and disk storage to support Monte Carlo calculations and data storage required for the analysis of top and photon plus jet channels. In particular, the photon + jet analysis has required substantial CPU power in order to utilize the results of various calculations.

Other needs involve the acquisition of peripherals such as tape storage compatible with that being used at the labs, the replacement of the current network technology with FDDI or some higher bandwidth alternative, and the use of RAID technology to decouple the processors from the local storage and provide higher bandwidth and reliability. A final goal is to spend some effort on remote interaction in light of the growing effort directed toward the ATLAS collaboration.

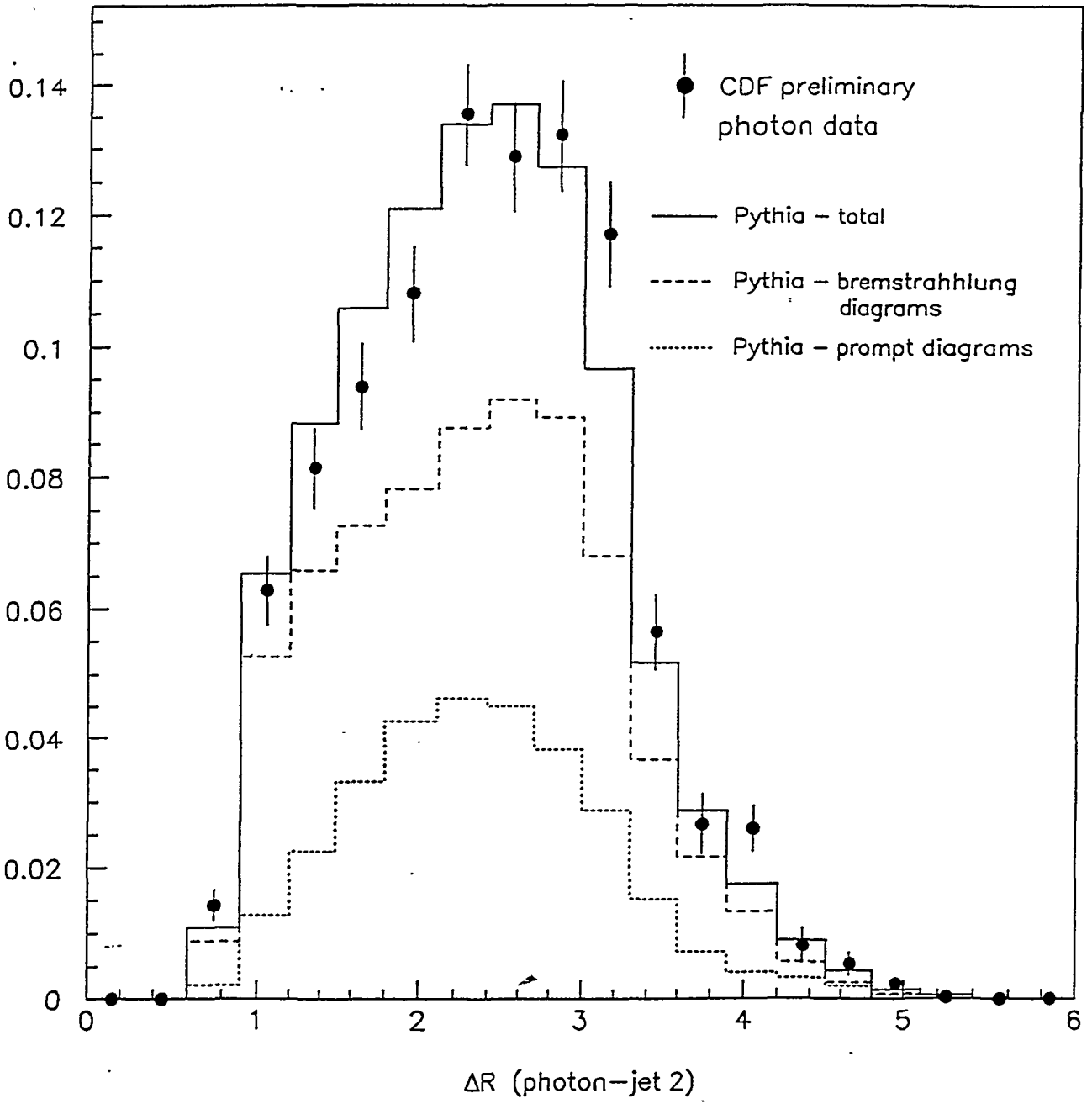

Figure 1 – $\eta - \phi$ Separation Between Photons and Low E_t Jets

Separation between the photon and lowest E_t jet, in photon + 2 jet events. This distribution is sensitive to the level of bremsstrahlung in prompt photon production. Points are CDF data. The prediction from the Pythia Monte Carlo (plus dectector simulation) is also shown (solid), as well as the components due to photon bremsstrahlung (dash) and non-bremsstrahlung (dot) processes. The presence of a bremsstrahlung component is necessary for agreement with data at small separation. This distribution has not been corrected for detector effects, and errors are statistical only.

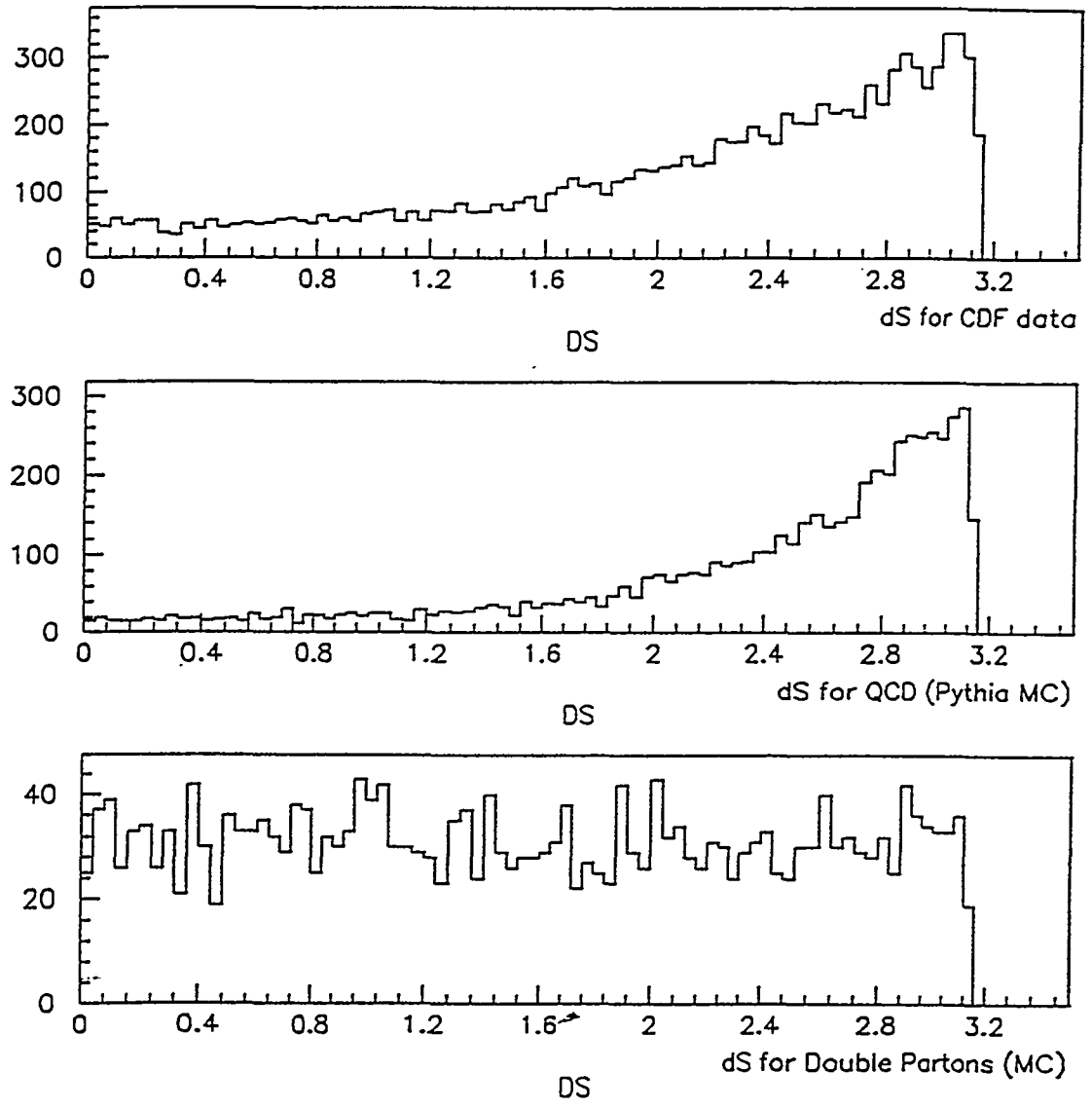

Figure 2 – δS-distributions of photon + 3 jet events

Azimuthal angle between the resulting P_t vectors for the photon-jet and di-jet pairs, in photon + 3 jet events. For Double Parton scattering this distribution is flat, while for single scattering a peak at π is expected (momentum conservation). Shown are results from CDF data (top), Pythia Monte Carlo (middle), and a Double Parton Monte Carlo. CDF data is best fit with an admixture of QCD and Double Parton events. These distribution have not been corrected for detector effects.

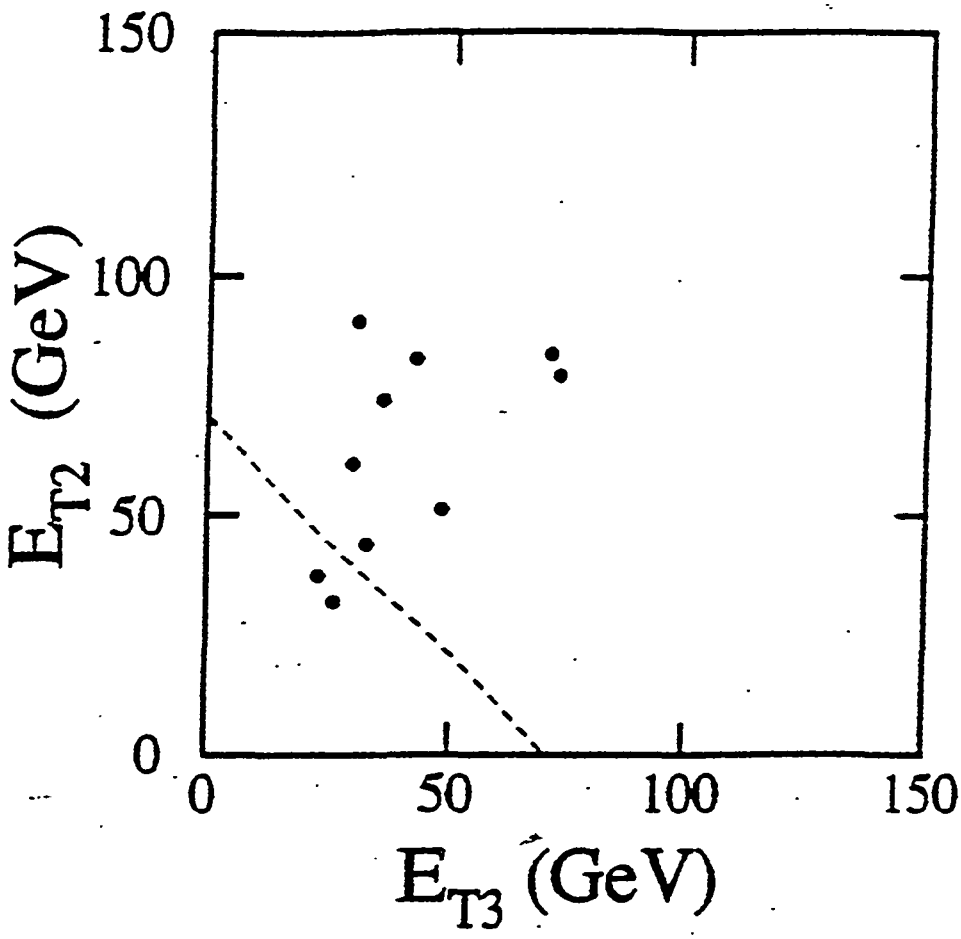

Figure 3 – Scatter Plot of Second and Third Highest E_T Jets in Top Events

Scatterplot of the transverse energy of the second E_t^2 and third E_t^3 highest E_t jets in top events. The dashed line divides the Monte Carlo sample into equally populated regions. In contrast, 8 of the 10 data events lie above the dashed line.

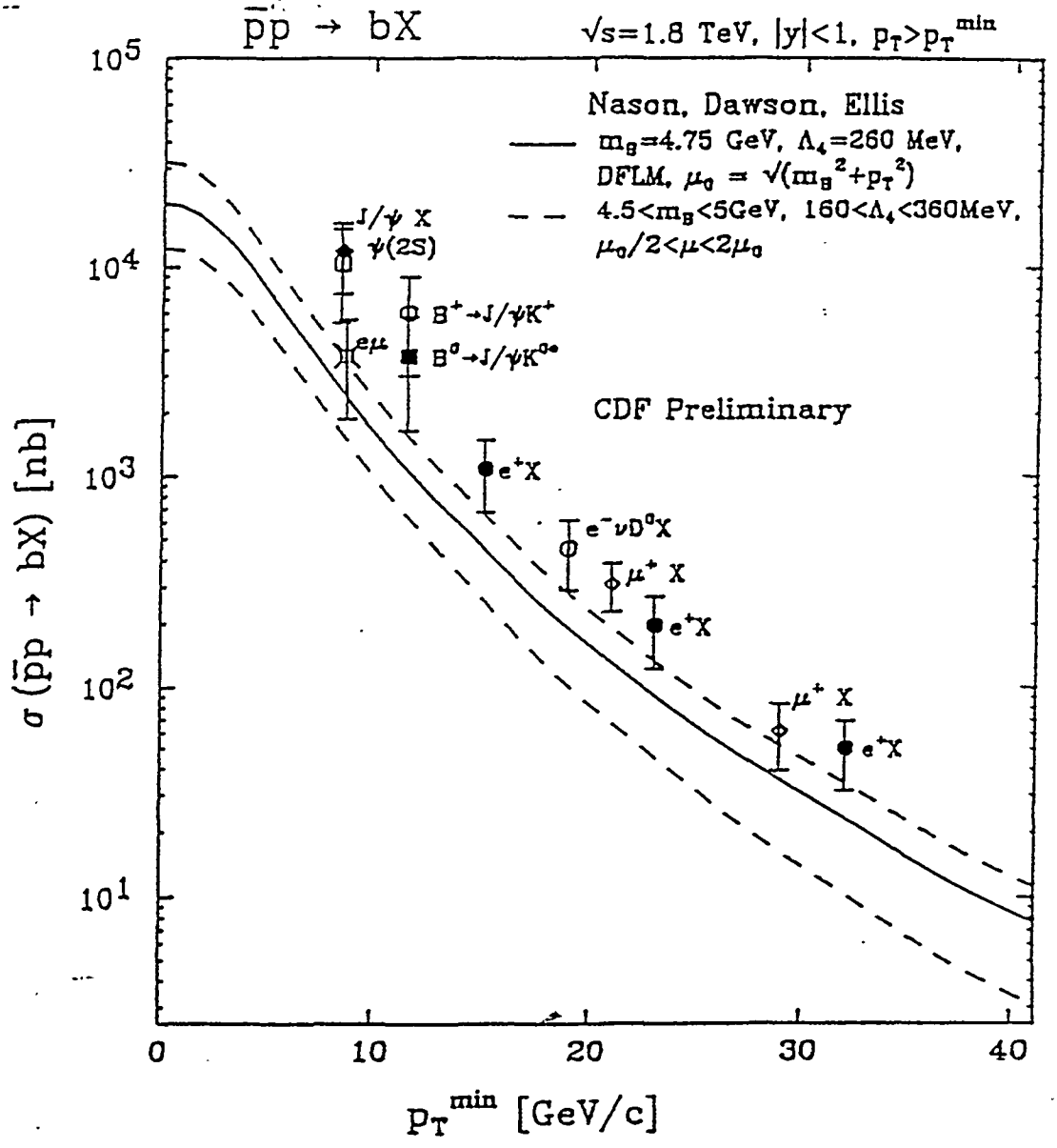

Figure 4 – Inclusive b Cross Section

Various measurements by CDF of the b quark cross section at the Tevatron, including the one deducted from the correlated $b\bar{b}$ events determined from $e\mu$ events. The solid line is the prediction from next-to-leading order QCD calculations and the dashed lines represent the theoretical uncertainty.

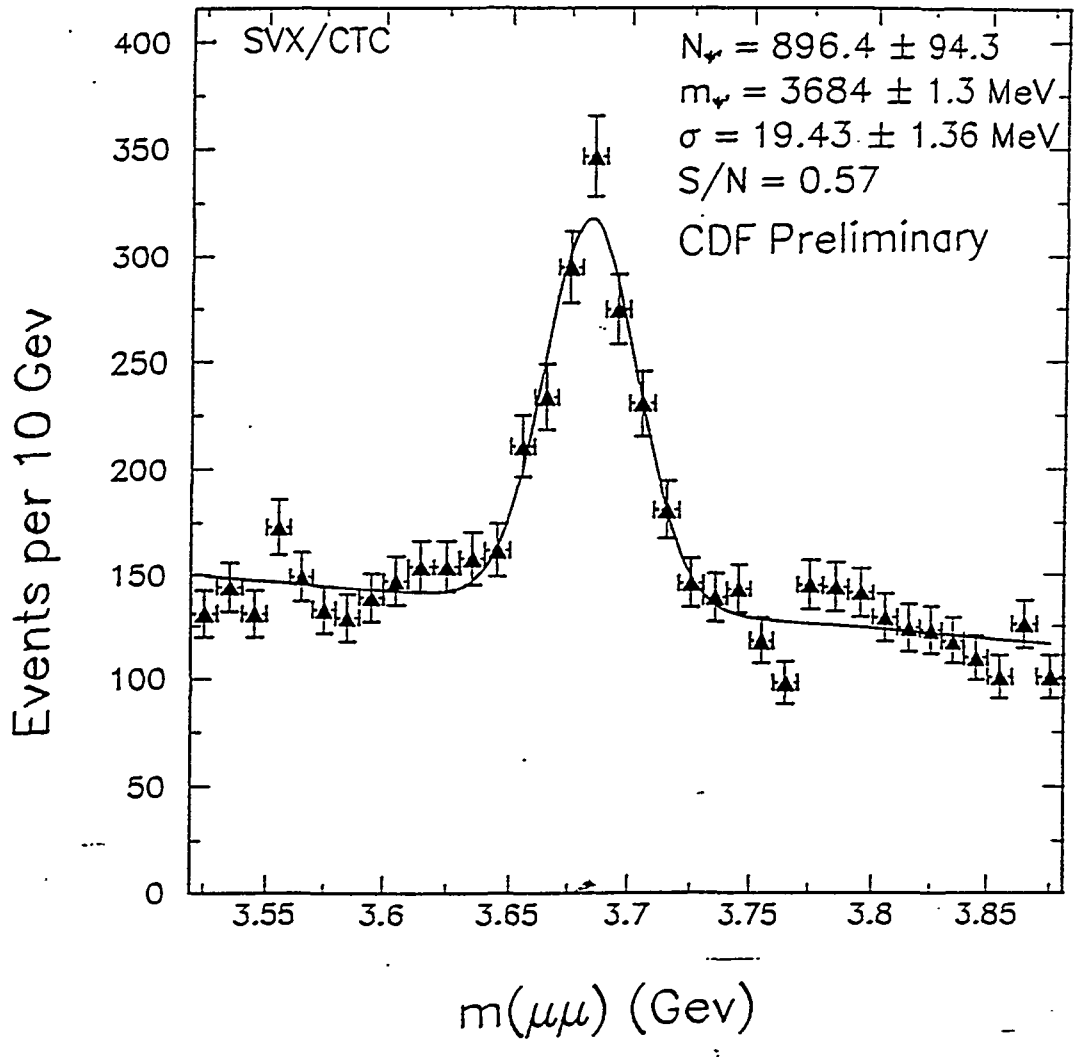

Figure 5 – $\mu^+\mu^-$ Invariant Mass Distribution in the ψ' Mass Region

Fitted invariant mass distribution of all μ^+/μ^- pairs in the ψ' mass region. The tracks are from both the CTC (central tracking) and SVX (silicon microvertex) detectors.

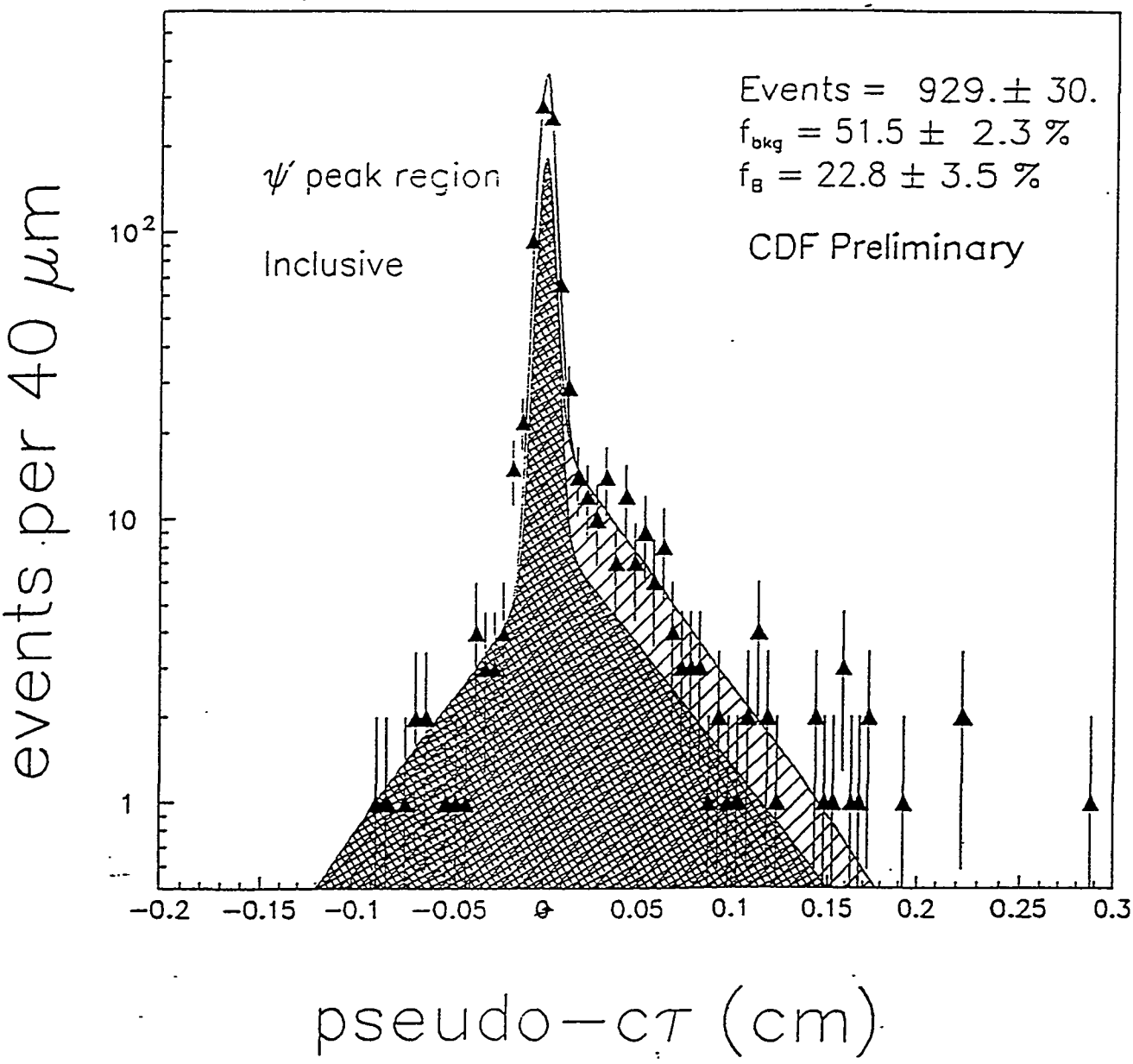

Figure 6 – Proper Time Distribution of ψ' Events

A fit of the proper time distribution of events that contain a ψ'. The shaded region is the background, while the hatched region represents the signal events. This plot is used to determine the fraction of ψ' decays that result from the decays of B's.

References

[1] CDF–1787: "Temperature and Pressure Monitoring for the Gas Calorimetry."

[2] CDF–2591: "The Gas Gain System for Run Ia (1992-1993)."

[3] CDF–1131: "Monte Carlo Fragmentation Tuning for Jet Energy and Resolution Analysis."

[4] CDF–1132: "Inclusive Jet E_t Spectrum: Energy Corrections and Resolution Unsmearing."

[5] CDF–1972, "The Two-Jet Differential Cross Section in 1992–1993 Data."

[6] CDF–2226, "Jet Results from the 1989 Data: New Energy Scale Definition."

[7] CDF–2378: "Kinematical Analysis of B-Tagged Events with Non-Gaussian Errors."

[8] FERMILAB-CONF-93/207-E, "The Ratio of CDF Low E_t Jet Cross Sections at $\sqrt{s} = 546$ & 1800 GeV."

[9] CDF–1286, "Central Calorimeter Pion Response in Light of 1990 Test Beam Data."

[10] CDF–1361, "Central Calorimeter Crack Response: 1990 Testbeam."

[11] CDF–1344, "Update on Central Calorimeter Response to Pions and Tuning of QFL."

[12] CDF–1650, "x_t Scaling (Updated)"

[13] CDF–1709, "Jet Scaling Update."

[14] CDF–2505, "ψ (2S) Cross Section and Production Mechanisms."

PUBLICATIONS

SDC Notes

SDC–93–461 "Impact of Timing Jitter and Pulse Height Variation on the SDC Calorimeter Energy Resolution"
Craig Blocker

SDC–93–462 "Mathematic Model of Calibrating the Calorimeter Using the Z_0 Mass Constraint"
Craig Blocker

SDC–93–463 "Effect of Tile-Ti-Tile Variations on the EM Calorimeter Resolution"
Craig Blocker and Marc Turcotte

SDC–93–535 "Muon Tube: Gas Leak Rate and Crimp Studies"
O. Remirez, D. Lorenzon, D. Kaplan, and Hermann Wellenstein

SDC–93–555 "A Simple Technique for Measurement of Wire Tension"
Larry Kirsch, D. Kaplan, and Hermann Wellenstein

SDC–93–560 "Effects of Mispositioning on the Level 1 Muon Trigger"
Steve Behrends and P. Hurst

SDT–000168 "Preliminary Design Report: Muon Barrel Toroid Support System"
J. Bensinger, *et al.*

SDT–000174 "SDC Muon Barrel Toroid Minutes: Magnet Engineering Meetings"
J. Bensinger, *et al.*

CDF Notes

CDF–2378 "Kinematical Analysis of B-Tagged Events with No-Gaussian Errors"
S. Behrends and K. Sliwa

CDF–2226 "Jet Results from the 1989 Data: New Energy Scale Definition"
S. Behrends

CDF–2196 "Proposal for a Special Run at $\sqrt{s} = 630$ GeV"
T. Lecompte, S. Kuhlmann, S. Behrends, B. Flaugher, J. Huth, and R. Plunkett

CDF–2158 "The Ratio of CDF Low ET Jet Cross-Sections at $\sqrt{s} = 546$ & 1800 GeV"
S. Behrends

CDF–2151 "The Ratio of Low ET Jet Cross-Sections at $\sqrt{s} = 546$ & 1800 GeV"
Steve Behrends

CDF–1972 "The Two-Jet Differential Cross-Section in 1992–1993 Data"
R. Plunkett, S. Behrends, and A. Bhatti

CDF–2623 "J/ψ, ψ' to $\mu\mu$ and B to J/ψ, ψ' Cross Sections"
G. Bauer, J. Cunningham, T. Daniels, P. Sphicas, N. Turini, V. Papadimitriou, The CDF Collaboration

CDF–2599 "J/ψ, ψ (2S) to $\mu\mu$ and B to J/ψ, ψ (2S) Cross Sections"
G. Bauer, J. Cunningham, T. Daniels, V. Papadimitriou, P. Sphicas, and N. Turini

CDF–2505 "ψ (2S) Cross Section and Production Mechanisms"
G. Bauer, J. Cunningham, T. Daniels, P. Sphicas

CDF–2268 "Study of the Jet ET Spectra in Lepton + Missing ET + 3 Jet Events"
Craig A. Blocker

CDF–2309 "A Measurement of the Botton Quark Cross Section Using Forward Muons"
Jodi Lamoureux

Publications from June 1, 1993 to May 31, 1994

1. "Evidence for Color Coherence in $p\bar{p}$ Collisions at $\sqrt{s} = 1.8$ TeV," F. Abe, *et al.*, The CDF Collaboration, submitted to Phys. Rev. D, March 22, 1994.

2. "Measurement of the B^+ and B^0 Lifetimes," F. Abe, *et al.*, The CDF Collaboration, submitted to Phys. Rev. Lett. January 25, 1994.

3. "Measurement of the Ratio $\sigma B(W \to e\nu)/\sigma B(Z \to e^+e^-)$ in $\bar{p}p$ Collisions at $\sqrt{s} = 1.8$ TeV," F. Abe, *et al.*, The CDF Collaboration, submitted to Phys. Rev. Lett. March 1, 1994.

4. "Search for Excited Quarks in $p\bar{p}$ Collisions at $\sqrt{s} = 1.8$ TeV," F. Abe, *et al.*, The CDF Collaboration, submitted to Phys. Rev. Lett. November 15, 1993.

5. "A Search for the Top Quark Decaying to a Charged Higgs in $p\bar{p}$ Collisions at $\sqrt{s} = 1.8$ TeV," F. Abe, *et al.*, The CDF Collaboration, submitted to Phys. Rev. Lett. November 12, 1993.

6. "Measurement of the Antiproton-Proton Total Cross Section at $\sqrt{s} = 546$ and 1800 GeV," F. Abe, *et al.*, The CDF Collaboration, submitted to Phys. Rev. D, August 3, 1993.

7. "Measurement of the $\bar{p}p$ Single Diffraction Dissociation at $\sqrt{s} = 546$ and 1800 GeV," F. Abe, *et al.*, The CDF Collaboration, submitted to Phys. Rev. D. August 3, 1993.

8. "Measurement of Small Angle Antiproton-Proton Elastic Scattering at $\sqrt{s} = 546$ and 1800 GeV," F. Abe, *et al.*, The CDF Collaboration, submitted to Phys. Rev. D, August 3, 1993.

9. "Measurement of the Average Lifetime of B-hadrons Produced in $p\bar{p}$ Collisions at $\sqrt{s} = 1.8$ TeV," F. Abe, *et al.*, The CDF Collaboration, Phys. Rev. Lett. 71, 3421 (1993).

10. "Observation of the Decay $B_s^0 \to J/\psi\phi$ in $\bar{p}p$ Collisions at $\sqrt{s} = 1.8$ TeV," F. Abe, *et al.*, The CDF Collaboration, Phys. Rev. Lett. 71, 1685 (1993).

11. "Search for Quark Compositeness, Axigluons and Heavy Particles using the Dijet Invariant Mass Spectrum Observed in $p\bar{p}$ Collisions," F. Abe, *et al.*, The CDF Collaboration, Phys. Rev. Lett. 71, 2542 (1993).

12. "A Measurement of the B Meson and b Quark Cross Sections at $\sqrt{s} = 1.8$ TeV Using the Exclusive Decay $B^0 \to J/\psi K^*(892)^0$," F. Abe, *et al.*, The CDF Collaboration, submitted to Phys. Rev. D, June 15, 1993.

13. "A Measurement of the Bottom Quark Production Cross Section in 1.8 TeV $p\bar{p}$ Collisions Using Muons from b-Quark Decays," F. Abe, *et al.*, The CDF Collaboration, Phys. Rev. Lett. 71, 2396 (1993).

14. "Inclusive χ_c and b-quark Production in $\bar{p}p$ Collisions at $\sqrt{s} = 1.8$ TeV," F. Abe, *et al.*, The CDF Collaboration, Phys. Rev. Lett. 71, 2537 (1993).

15. "A Search for First-Generation Leptoquarks in $\bar{p}p$ Collisions at $\sqrt{s} = 1.8$ TeV at CDF," F. Abe, *et al.*, The CDF Collaboration, Phys. Rev. D, Rapid Communications, 48, R3939 (1993).

16. "A Measurement of Jet Multiplicity in W Events Produced in $\bar{p}p$ Collisions at $\sqrt{s} = 1.8$ TeV," F. Abe, *et al.*, The CDF Collaboration, Phys. Rev. Lett. 70, 4042 (1993).

17. "The Center-of-Mass Angular Distribution from Prompt Photons Produced in $p\bar{p}$ Collisions at $\sqrt{s} = 1.8$ TeV," F. Abe, *et al.*, The CDF Collaboration, Phys. Rev. Lett. 71, 679 (1993).

18. "A Study of Four-Jet Events and Evidence for Double Parton Interactions in $p\bar{p}$ Collisions at $\sqrt{s} = 1.8$ TeV," F. Abe, *et al.*, The CDF Collaboration, Phys. Rev. **D**, 47, 4857 (1993).

19. "Measurement of the Cross Section for Production of Two Isolated Prompt Photons in $p\bar{p}$ Collisions at $\sqrt{s} = 1.8$ TeV," Phys. Rev. Lett. 70, 2232 (1993).

20. "A Prompt Photon Cross Section Measurement in $\bar{p}p$ Collisions at $\sqrt{s} = 1.8$ TeV," F. Abe, *et al.*, The CDF Collaboration, Phys. Rev. **D**, 48, 2998 (1993).

21. "Measurement of the Dijet Mass Distribution in $p\bar{p}$ Collisions at $\sqrt{s} = 1.8$ TeV," F. Abe, *et al.*, The CDF Collaboration, Phys. Rev. **D**, 48, 998 (1993).

22. "Search for $\Lambda_b \rightarrow J/\psi\Lambda^0$ in $p\bar{p}$ Collisions at $\sqrt{s} = 1.8$ TeV," F. Abe, *et al.*, The CDF Collaboration, Physical Review **D**, 47, Rapid Communications 47, R2639 (1993).

23. "Comparison of Jet Production in $\bar{p}p$ Collisions at $\sqrt{s} = 546$ and 1800 GeV," F. Abe, *et al.*, The CDF Collaboration, Phys. Rev. Lett. 70, 1376 (1993).

THEORY

During the past year, the theoretical physics group pursued research in quantum field theory, with the $1/N$ expansion and other non-perturbative methods providing a unifying theme of much of this work. The research was carried out by Prof. Schnitzer, Dr. Riggs, Mr. Mlawer and Mr. Nunes, and in part in collaboration with Dr. Naculich of Bowdoin College.

1. RESEARCH ACTIVITIES

1.1 Large N Limit in Scalar Field Theory

The possibility of a strongly interacting Higgs sector, with large Higgs mass, has motivated methods which can deal with the interactions of scalars that are non-perturbative in the coupling constant. One approach to this issue is to reorganize the theory in terms of some other expansion parameter, such as the $1/N$ expansion for a theory with internal symmetry such as O(4), continued to O(N) for example. Predictions are then obtained by evaluating results of the expansion at the physical value of N (N=4 say). The $1/N$ expansion for $\lambda\phi^4$ theory (in 3+1 dimensions) with O(N) symmetry (the so-called vector model) has been extensively studied as a renormalized field theory. However, the renormalized vector model encounters a number of problems. Among these, discussed some time ago by Abbott, Kang, and Schnitzer, are:
1) The effective potential of the theory is double valued, with the lower energy branch of the potential describing a phase of the theory with unbroken internal symmetry, *i.e.*, $< \Phi_a >= 0$. This phase is tachyon free in all orders of the $1/N$ expansion. The higher energy branch of the effective potential does allow a spontaneously broken symmetry. However, this phase contains tachyons, presumably as a symptom of decay to the lower energy phase. In higher orders of the $1/N$ expansion, the higher energy branch of the effective potential becomes everywhere complex.
2) The effective potential has no lowest energy bound as the external field $\phi \to \infty$. The tachyon-free phase (*i.e.*, with $< \Phi_a >= 0$) of the $1/N$ expansion tunnels non-perturbatively to this unstable vacuum, with an amplitude proportional to exp(−N). The tachyon free phase is a metastable state, but is unsuitable for phenomenology, as it does not support spontaneous symmetry breaking.
3) It is widely believed that $\lambda\phi^4$ theory in 4–dimensions is actually a trivial, free-field theory, which may be at the root of the problems summarized above.

One possible way to deal with these problems is to consider a cutoff version of the vector model in the $1/N$ expansion. One introduces a cutoff Λ into the theory, which represents a mass-scale above which the self-coupled Higgs sector can no longer be considered isolated from other essential degrees of freedom of a more complete theory. There are other possible interpretations of the cutoff, particularly if the Higgs is not elementary, but only represents a scalar bound-state of some effective field theory. However, one does not need to commit oneself to any particular physical interpretation of the cutoff.

A number of results for the cutoff vector model in the large N limit are already available. However, a thorough understanding of the effective potential often gives new insights into the behavior of a field theory. Nunes and Schnitzer gave a careful presentation of the effective potential to leading order in 1/N for the cutoff vector model. They found that the effective potential was surprisingly rich in structure, with several phases possible, depending on the parameters of the model. Some restrictions

on the parameters and external field strengths were required to obtain a phenomenologically viable model for energies $< \Lambda$. With such restrictions they found a phenomenologically acceptable model with spontaneously broken symmetry, a potential bounded below, and amplitudes free of tachyons, which is consistent with earlier phenomenological analyses. The resonance structure of meson-meson scattering in the $O(N-1)$ singlet sector in this phase was studied. The scattering amplitude exhibits a resonance which can be interpreted as the Higgs meson of the model, in weak as well as in strong coupling. There is also an unphysical resonance above the cutoff mass Λ, which was interpreted as defining the triviality mass-scale of the theory.

As an application of the analysis of the effective potential, Nunes and Schnitzer considered the possibility of a double-scaling limit for this cutoff model. It was shown that the double-scaling limit does not exist for the cutoff vector model.

1.2 Two-Dimensional Yang–Mills Theories

Calculations for hadron physics from QCD remains tantalizingly elusive after nearly two decades of effort. The strong interactions exhibit string characteristics at low momentum transfers, and this provided the original impetus for the development of string theory as a theory of hadrons. Formulating QCD as a string theory would be an important step in connecting it to hadron physics, and perhaps in explaining confinement.

At present it is still difficult to address these issues in four-dimensions. In an important series of papers, Gross, Gross–Taylor, and Minahan have turned to 2-dimensional QCD in the hope of generating new ideas applicable to four dimensions.

These authors argued that two-dimensional QCD is a string theory. They showed that the $1/N$ expansion of the partition function for two-dimensional $SU(N)$ gauge theories without fermions on an orientable manifold $\mathcal{M}$ can be associated with maps from a genus expansion of string world-sheets to Euclidean space-time $\mathcal{M}$. The string theory is determined by the set of world-sheets to be included in the genus expansion, the types of maps counted, and the weights of these maps in the $1/N$ expansion of the $SU(N)$ Yang–Mills partition function.

Naculich, Riggs, and Schnitzer showed that two-dimensional $SO(N)$ and $Sp(N)$ Yang–Mills theories without fermions can also be interpreted as closed string theories. The terms in the $1/N$ expansion of the partition function on an orientable or nonorientable manifold $\mathcal{M}$ can be associated with maps from a string worldsheet onto $\mathcal{M}$. These maps are unbranched and branched covers of $\mathcal{M}$ with an arbitrary number of infinitesimal worldsheet cross-caps mapped to points in $\mathcal{M}$. These string theories differ from $SU(N)$ Yang–Mills string theory in that they involve odd powers of $1/N$ and therefore require both orientable and nonorientable worldsheets. Ramgoolam has also contributed to the string picture of two-dimensional $SO(N)$ and $Sp(N)$ Yang–Mills theories.

Thus the long-anticipated connection between large N QCD and string theory has now been made precise for two-dimensional Yang–Mills theory with gauge groups $SU(N)$, $SO(N)$, and $Sp(N)$. The leading terms in the $1/N$ expansion count topologically distinct (unbranched) coverings of $\mathcal{M}$ by the string worldsheets. The primary subleading terms correspond to coverings with simple branch points as well as (branched and unbranched) coverings that map infinitesimal handles (for $SU(N)$) or infinitesimal cross-caps (for $SO(N)$ and $Sp(N)$) on the worldsheet to points on $\mathcal{M}$. When $\mathcal{M}$ is not a torus or Klein bottle (so that the Euler characteristic of $\mathcal{E}$ of $\mathcal{M}$ is nonzero), additional subleading terms arise that have properties reminiscent of coverings with multiple branch points.

While these so-called *twist-point* terms do produce permutations of the sheets of the covering, as would be expected if the twist points were multiple branch points, they have another property that had presented a puzzle for this interpretation. Namely, while each simple branch point term appears with a single power of the area of $\mathcal{M}$, twist point terms do not carry any powers of the area (despite the fact that multiple branch points are homotopically equivalent to a confluence of simple branch points).

For the geometric interpretation of Yang–Mills theory to be viable, each of the terms in the partition function expansion must correspond to an actual covering of some sort. For example, Kneser's theorem states that nonconstant continuous maps from a Riemann surface of genus g (with $\mathcal{E}_g = 2 - 2g$) to a Riemann surface of genus G (with $\mathcal{E}_G = 2 - 2G$) do not exist if

$$\mathcal{E}_g > r\mathcal{E}_G$$

where r is the degree of the map. The same constraint holds for orientation-true maps between nonorientable surfaces. Remarkably, no terms arise in the Yang–Mills partition function that violate these constraints, as demonstrated by the work cited above.

Naculich, Riggs, and Schnitzer considered another restriction on the terms of the Yang–Mills partition function. It is a topological (rather than complex-analytic) fact that the total number of branch points (counted with multiplicity) must be even for any branched covering of an orientable or nonorientable surface without boundary. The factor of $\mathcal{A}$ associated with each simple branch point term is interpreted as the integration of the location of the ramification points (those covering the branch points on $\mathcal{M}$) over the worldsheet. Naculich, Riggs, and Schnitzer showed that the total branch point multiplicity can only be even if the twist points are interpreted as multiple branch points. This interpretation therefore seems to be essential for the consistency of the string interpretation. From the vantage point of Yang–Mills theory on both orientable and nonorientable surfaces, the evenness of multiplicity constraint is enforced by the transposition symmetry of the theory. This result is non-trivial, particularly for $\mathrm{SO}(N)$ and $\mathrm{Sp}(N)$, as the area dependent terms can appear with odd powers of $1/N$.

In pure two-dimensional Yang–Mills theory, Wilson loop expectation values are the only observables. These Wilson loop expectation values for $\mathrm{SU}(N)$ gauge theory on orientable surfaces are known exactly in the gauge theory context. Gross and Taylor showed that Wilson loop expectation values for $\mathrm{SU}(N)$ have a string interpretation as well; the result being closely related to a string theory on a worldsheet with boundary.

Naculich, Riggs, and Schnitzer have shown in detail how Wilson loops in $\mathrm{SO}(N)$ and $\mathrm{Sp}(N)$ two-dimensional Yang–Mills theory on any (orientable or non-orientable) surface have a natural interpretation as a weighted sum of covers of that surface. These results, and that of Gross and Taylor, reinforces the idea that the large N expansion and two-dimensional gauge theories can be reproduced by a string theory. It is also shown how the results of Gabai and Kazez on classifying non-orientable surfaces fit into this program.

PUBLICATIONS
From June 1, 1993 to May 31, 1994

Large N Limit in Scalar Field Theory

1. "The Cutoff $\lambda\phi^4$ O(N) Model in the Large N Limit" (Nunes and Schnitzer), Brandeis preprint BRX–TH–351, hep-ph/9311319, 30 pages, submitted for publication.

Two-Dimensional Yang–Mills Theory

2. "Two-Dimensional Yang–Mills Theories are String Theories" (Naculich, Riggs, and Schnitzer), Modern Physics Letters **A8**, 2223–2235 (1993).

3. "Twist-Points as Branch Points for for the QCD_2 String" (Naculich, Riggs, and Schnitzer), Physics Letters **B319**, 466–470 (1993).

4. "The String Calculation of Wilson Loops in SO(N) and Sp(N) Yang–Mills Theory" (Naculich, Riggs, and Schnitzer), Brandeis preprint BRX–TH–355, hepth94 06100.

Integrable Two-Dimensional Field Theories

5. "Integrable N=2 Landau–Ginzburg Theories from Quotients of Fusion Rings" (Mlawer, Riggs, and Schnitzer), Nuclear Physics **B418**, 603–634 (1994).

Ph.D. Thesis

6. "Topological N=2 Landau–Ginzburg Theories from $Sp(N)_K$ and $SO(N)_K$ Fusion Rings" April 1994 (Mlawer), 80 pages.

Book Review

7. "Supersymmetry and Supergravity" by J. Wess and J. Bagger in Classical and Quantum Gravity **10**, 2448 (1993) (Schnitzer).